Nonlinear wave propagation in porous materials based on the Biot theory

L. H. Tong, Y. S. Liu, D. X. Geng, and S. K. Lai

ARTICLES YOU MAY BE INTERESTED IN

Theory of Propagation of Elastic Waves in a Fluid-Saturated Porous Solid. I. Low-Frequency Range
The Journal of the Acoustical Society of America **28**, 168 (1956); https://doi.org/10.1121/1.1908239

Theory of Propagation of Elastic Waves in a Fluid-Saturated Porous Solid. II. Higher Frequency Range
The Journal of the Acoustical Society of America **28**, 179 (1956); https://doi.org/10.1121/1.1908241

Mechanics of Deformation and Acoustic Propagation in Porous Media
Journal of Applied Physics **33**, 1482 (1962); https://doi.org/10.1063/1.1728759

Nonlinear acoustic waves in porous media in the context of Biot's theory
The Journal of the Acoustical Society of America **102**, 2521 (1997); https://doi.org/10.1121/1.421011

Propagation of pore pressure diffusion waves in saturated porous media
Journal of Applied Physics **117**, 134902 (2015); https://doi.org/10.1063/1.4916805

Acoustic wave propagation through porous media: Theory and experiments
The Journal of the Acoustical Society of America **102**, 2495 (1997); https://doi.org/10.1121/1.420304

Across Acoustics
The official podcast highlighting authors' research from our publications

Nonlinear wave propagation in porous materials based on the Biot theory

L. H. Tong,[1] Y. S. Liu,[2] D. X. Geng,[1] and S. K. Lai[3,a]

[1]*Jiangxi Key Laboratory of Infrastructure Safety and Control in Geotechnical Engineering, East China Jiaotong University, Nanchang, Jiangxi, People's Republic of China*

[2]*Institute of Engineering Mechanics, School of Civil Engineering and Architecture, East China Jiaotong University, Nanchang, Jiangxi, People's Republic of China*

[3]*Department of Civil and Environmental Engineering, The Hong Kong Polytechnic University, Hung Hom, Kowloon, Hong Kong, People's Republic of China*

Nonlinearity must be considered with some porous granular media because of the large deformation under seismic waves. In this study, the propagation of nonlinear waves in porous media is studied based on the Biot theory and the governing equations are obtained by the Lagrangian formulation. Three new nonlinear parameters are introduced to consider the coupled nonlinearity between the solid and fluid components in porous media. It is shown that an additional nonlinear wave with a double frequency is generated by the coupling effect of linear fast and slow waves. When only a shear wave is applied at the source, no double-frequency nonlinear wave is predicted and three nonlinear longitudinal waves are generated. On the basis of the practical case studies, the effect of strong nonlinearity is computed under the influence of a one-dimensional single longitudinal wave source and a single shear wave source. © 2017 Acoustical Society of America.
[http://dx.doi.org/10.1121/1.4996439]

I. INTRODUCTION

Porous materials are frequently found in many engineering fields, such as soils, rocks, and gassy sediments in geophysical engineering, earthquake engineering and oceanographic engineering (Solovev, 1990; Meegan *et al.*, 1993; Johnson and Jia, 2005; Johnson *et al.*, 2008; Pushkina, 2012). Moreover, porous metals have also been successfully used for the fabrication of acoustic liners in aero-engines (Ashby, 2006; Wang *et al.*, 2009). The linear poroelasticity theory proposed by Biot (1956a,b, 1962) has been intensively used to investigate porous materials since its experimental verification in 1980 by Plona, who observed a slow compressional wave (Plona, 1980). A considerable number of works on the low-amplitude wave propagation characteristics of saturated porous materials have also been reported (Cui *et al.*, 2003; Liu *et al.*, 2005; Sharma, 2007; Bouzidi and Schmitt, 2009; Cui *et al.*, 2010; Papargyri-Beskou *et al.*, 2012; Tao *et al.*, 2014; Yang *et al.*, 2015; Tong *et al.*, 2016). In recent years, the increasing interest in various applications of nonlinearity in porous materials has attracted the attention of researchers. For example, porous metals have demonstrated great potential as sound absorbers at high sound pressure levels (Zhang *et al.*, 2012). Granular materials, including soils, rocks and gassy sediments, are other examples of typical porous materials that show a higher degree of nonlinearity than water due to their structural inhomogeneity. As a result, the characteristics of nonlinearity can be used to investigate porous material properties. Whilst the characteristics of nonlinear acoustic waves propagating in granular materials have found use in oil prospecting and ecological monitoring in ocean sediments (Kim and Yoon, 2009), few studies on the characteristics of nonlinear wave propagation in saturated porous materials have been performed.

In an early effort, Biot developed a nonlinear and semi-linear theory of porous solids in terms of the Cartesian definition of finite strains and local rotation fields (Biot, 1973). Nonlinear behaviour, according to Biot (1973), is affected by both local geometric effects (e.g., crack closure, contact area) and physical properties. Under this consideration, seven physical constants were introduced to describe the semi-linear properties, in which the stress-strain relationship was expressed in a particular form for an isotropic porous material. This nonlinear and semi-linear rheology has been successfully applied by Rice to investigate the stability of dilatant hardening for saturated rock masses (Rice, 1975). Making use of a variational formulation, Berryman and Thigpen (1985) established a set of nonlinear equations for wave propagation in dry or fluid-saturated porous materials under the Lagrangian reference frame, in which the micro-inertia terms accounted for the density fluctuations of fluids and solids. Unlike the phenomenological Biot theory, which was derived by the intuitive extension of existing theories, this theory was proposed from a more theoretical point of view. Various formulations for the simulation of porous materials based on the mixture theory have been implemented, and the nonlinear constitutive equations to describe large strains along with the corresponding dissipative mechanisms have also been derived (Borja and Alarcón, 1995; Wilmanski, 1996; Kempa, 1997). Furthermore, the thermodynamic formulation for a porous medium saturated with a

a)Electronic mail: sk.lai@polyu.edu.hk

compressible fluid that undergoes large elastic and plastic deformations has been presented in accordance with the mixture theory (Larsson and Larsson, 2002). Other theories for investigation of nonlinear wave propagations in porous materials can also be found in the literature, such as the porosity dynamic theory proposed by Lopatnikov and Cheng (2004), in which porosity was introduced as an independent variable to characterise the behaviour of porous materials.

The literature only describes a few experiments aimed at the observation of nonlinear effects and the estimation of nonlinear parameters (Moussatov *et al.*, 2001; Kim and Yoon, 2009; Legland *et al.*, 2012). Moussatov *et al.* (2001) experimentally observed the self-demodulation effect of ultrasonic waves due to nonlinear processes in granular media. A parametric acoustic array theory was later used by Kim and Yoon (2009) to estimate the nonlinear parameter of water-saturated sandy sediments. The corresponding measured nonlinear parameter for the water-saturated sandy sediment was around 80 at a difference frequency of 38 kHz, which is much higher than that in water. In addition, experiments on the second harmonic generation using a granular medium slab were conducted by Legland *et al.* (2012), and the results again compared well with the theoretical prediction from the Biot wave model.

Although various theories have been developed with rigorous derivations for the dynamic response analysis of porous materials, they are non-intuitive and mathematically complicated. Hence, the applicability and flexibility of these theories in real engineering practice are limited. In this connection, the Biot theory is probably the most widely used model for the analysis of dynamic characteristics in porous materials. For instance, Dazel and Tournat (2010) applied the Biot theory to model nonlinear wave propagation in porous materials and also extended its application to granular media. Their analysis revealed the thermal and viscous effects on fluid and solid motions along with the inertial and elastic couplings between the solid and fluid components. The nonlinear stresses in both solid and fluid phases under different frequencies were also investigated. Following the nonlinear Biot theory, Donskoy *et al.* (1997) studied nonlinear waves in a porous medium by introducing porosity-dependent structure parameters. The effective nonlinear parameter was theoretically determined. In fact, only three nonlinear parameters were introduced to describe the cubic nonlinear potential in the nonlinear Biot theory (Biot, 1973). However, it is well known that even for a purely isotropic elastic solid, three nonlinear parameters already exist in the cubic nonlinear potential. This implies that, in the nonlinear Biot theory, porous materials are viewed as a statistically isotropic pure material. Therefore, the solid-fluid coupling nonlinear parameters are missing in the expression of the nonlinear potential in the nonlinear Biot theory developed by Donskoy *et al.* (1997).

In this paper, three new nonlinear parameters are first introduced to completely describe the nonlinear potential without any additional assumptions. The coupled nonlinear wave propagation equations are obtained based on the new nonlinear potential expression using the Lagrangian formulation. The effect of the second harmonic wave generation in porous materials is also analysed under a one-dimensional configuration in an infinite medium.

II. GOVERNING EQUATIONS IN SATURATED POROUS MATERIALS

Consider a representative elementary volume Ω bounded by a surface S, within which a point is designated by $\mathbf{a} = (a, b, c)$ in an undeformed configuration. When an external disturbance occurs, this point is shifted to a new location designated by $\mathbf{x} = (x, y, z)$. Then, the deformation gradient tensor can be written as

$$\mathbf{F} = \frac{\partial \mathbf{x}}{\partial \mathbf{a}} = \begin{bmatrix} \dfrac{\partial x}{\partial a} & \dfrac{\partial x}{\partial b} & \dfrac{\partial x}{\partial c} \\ \dfrac{\partial y}{\partial a} & \dfrac{\partial y}{\partial b} & \dfrac{\partial y}{\partial c} \\ \dfrac{\partial z}{\partial a} & \dfrac{\partial z}{\partial b} & \dfrac{\partial z}{\partial c} \end{bmatrix}. \tag{1}$$

Introducing another tensor defined as

$$\varepsilon = \frac{1}{2}(\mathbf{F}^T \cdot \mathbf{F} - \mathbf{I}), \tag{2}$$

where $\mathbf{F}^T$ is the transposed tensor of $\mathbf{F}$ and $\mathbf{I}$ is the two-order unit tensor. It is easily proved that the tensor ε is a strain tensor in the Lagrangian formulation. If the studied point is located on a solid component, then $\mathbf{F}$ and ε are the solid deformation gradient tensor and strain tensor, respectively. The displacement of the solid matrix is designated by $\mathbf{u} = (u_1, u_2, u_3)$ and the average fluid displacement is $\mathbf{U} = (U_1, U_2, U_3)$. We further define $\mathbf{w} = n_0(\mathbf{U} - \mathbf{u})$ with n_0 the porosity to describe the flow of fluids relative to solids. Following the elaboration of Biot's work (Biot, 1962), in a statistically isotropic medium, the strain energy Φ is a function of three invariants I_1, I_2, I_3 of the solid strain tensor and the variable ζ:

$$\Phi = \Phi(I_1, I_2, I_3, \zeta), \tag{3}$$

where $I_1 = \varepsilon_{ii}$, $I_2 = \varepsilon_{11}\varepsilon_{22} + \varepsilon_{11}\varepsilon_{33} + \varepsilon_{22}\varepsilon_{33} - \varepsilon_{12}\varepsilon_{21} - \varepsilon_{13}\varepsilon_{31} - \varepsilon_{23}\varepsilon_{32}$, $I_3 = |\varepsilon|$, and $\zeta = -\text{div}\,\mathbf{w} = n_0\text{div}(\mathbf{u} - \mathbf{U})$ with an assumption of uniform porosity, in which $\text{div}(\cdot)$ is the divergence operator in a reference formulation. Physically, the variable ζ represents the increment of fluid content. Additional cubic potential terms are introduced to the strain energy to characterise the nonlinearity. In this case, the strain energy can be written as

$$\Phi = \overbrace{\frac{\lambda_c + 2\mu}{2}I_1^2 - 2\mu I_2 - \alpha M I_1 \zeta + \frac{1}{2}M\zeta^2}^{\text{Linear terms}}$$
$$+ \underbrace{\frac{1}{3}(l + 2m)I_1^3 - 2m I_1 I_2 + n I_3 + \gamma_2 I_1^2 \zeta + \gamma_3 I_1 \zeta^2 + \gamma_1 \zeta^3}_{\text{Nonlinear terms}}. \tag{4}$$

The linear terms are directly inherited from the expression of Biot's work (Biot, 1962). Hence, these parameters in the linear terms have the same definitions as those mentioned in Biot's work (Biot, 1962). Six parameters are introduced to the nonlinear terms, three more terms than those in the nonlinear Biot theory (Biot, 1973). In the above equation, l, m, and n are the

nonlinear elastic constants related to the solid components. The constant γ_1 is related to the fluid phase, while γ_2 and γ_3 are used to reveal the nonlinear coupled properties between the solid components and fluid contents. We observe that these six nonlinear constants can completely determine the cubic nonlinear properties in fluid saturated porous materials.

There are two types of dissipative processes in a porous medium (Lopatnikov and Cheng, 2004). One is the process in which dissipation occurs even without the physical movement of materials, such as mass diffusion and relaxation of temperature. The other process is related to the movement that is irreversible. For mathematical simplicity, only the second dissipative process is considered in this work. In an isotropic medium, the dissipation function is given by (Biot, 1962)

$$D = \frac{\eta}{2\kappa} \dot{\mathbf{w}} \cdot \dot{\mathbf{w}}^T, \tag{5}$$

where $\dot{\mathbf{w}}^T$ is the transposed vector of $\dot{\mathbf{w}}$, η is the fluid viscosity, and κ is the coefficient of permeability.

For a unit volume of bulk materials, by using the variables $\mathbf{u}$ and $\mathbf{w}$, the kinetic energy can be written as (Biot, 1962)

$$T = \frac{1}{2}\rho\dot{\mathbf{u}} \cdot \dot{\mathbf{u}}^T + \frac{1}{2}m'\dot{\mathbf{w}} \cdot \dot{\mathbf{w}}^T + \rho_f \dot{\mathbf{w}} \cdot \dot{\mathbf{u}}^T, \tag{6}$$

where ρ and ρ_f are, respectively, the mass densities of the bulk material and the pore fluid; $m' = \alpha\rho_f/n_0$ with α the material parameter (Biot, 1941, 1962); and $\rho = (1 - n_0)\rho_s + n_0\rho_f$ with ρ_s the mass density of the solid. On the basis of the above equations, the Lagrangian for a system of porous materials is defined by

$$L = T + \Phi. \tag{7}$$

Besides, the equations of motion of a dissipative system can be derived by the Lagrangian equation as

$$\frac{d}{dt}\left(\frac{\partial L}{\partial \dot{q}_i}\right) - \frac{\partial L}{\partial q_i} + \frac{\partial D}{\partial \dot{q}_i} = 0. \tag{8}$$

Considering $\mathbf{u}$ and $\mathbf{w}$ as generalized coordinates and substituting Eq. (7) into Eq. (8), we obtain

$$\frac{\partial \Phi}{\partial \mathbf{u}} = \frac{d}{dt}\left(\frac{\partial T}{\partial \dot{\mathbf{u}}}\right),$$
$$\frac{\partial \Phi}{\partial \mathbf{w}} = \frac{d}{dt}\left(\frac{\partial T}{\partial \dot{\mathbf{w}}}\right) + \frac{\partial D}{\partial \dot{\mathbf{w}}}. \tag{9}$$

If we define $\mathbf{x}$ as a solid point in the deformed formulation, then $\mathbf{u} = \mathbf{x} - \mathbf{a}$. Therefore, we have $d\mathbf{u} = d\mathbf{x}$. The terms $\partial\Phi/\partial\mathbf{u}$ and $\partial\Phi/\partial\mathbf{w}$ can be expressed in a component form as follows:

$$\frac{\partial \Phi}{\partial \mathbf{u}} = \frac{d}{da_k}\left[\frac{\partial \Phi}{\partial \varepsilon_{jl}}\frac{\partial \varepsilon_{jl}}{\partial\left(\frac{\partial x_i}{\partial a_k}\right)}\right],$$
$$\frac{\partial \Phi}{\partial \mathbf{w}} = \frac{d}{da_k}\left[\frac{\partial \Phi}{\partial \zeta}\frac{\partial \zeta}{\partial\left(\frac{\partial w_i}{\partial a_k}\right)}\right]. \tag{10}$$

Consider $\varepsilon_{ij} = \frac{1}{2}\left[(\partial x_k/\partial a_i)\,(\partial x_k/\partial a_j) - \delta_{ij}\right]$ and $\zeta = -\mathrm{div}\mathbf{w}$, then

$$\frac{\partial \varepsilon_{jl}}{\partial\left(\frac{\partial x_i}{\partial a_k}\right)} = \frac{1}{2}\left(\delta_{jk}\frac{\partial x_i}{\partial a_l} + \delta_{lk}\frac{\partial x_i}{\partial a_j}\right),$$
$$\frac{\partial \zeta}{\partial\left(\frac{\partial w_i}{\partial a_k}\right)} = -\mathbf{I}. \tag{11}$$

Substituting Eq. (11) into Eq. (10) yields

$$\frac{\partial \Phi}{\partial \mathbf{u}} = \frac{d}{da_k}\left[F_{il} \cdot \frac{\partial \Phi}{\partial \varepsilon_{kl}}\right] = \left(\mathbf{F} \cdot \frac{\partial \Phi}{\partial \boldsymbol{\varepsilon}}\right) \cdot \overleftarrow{\nabla},$$
$$\frac{\partial \Phi}{\partial \mathbf{w}} = \frac{d}{da_k}\left[-I_{jk} \cdot \frac{\partial \Phi}{\partial \zeta}\right] = \left(-\mathbf{I} \cdot \frac{\partial \Phi}{\partial \zeta}\right) \cdot \overleftarrow{\nabla}, \tag{12}$$

where $\overleftarrow{\nabla}$ is the divergence operator in the Lagrangian formulation and $\mathbf{F}$ is the deformation gradient tensor of the solid component. From Eq. (4), we have

$$\frac{\partial \Phi}{\partial \boldsymbol{\varepsilon}} = \left[(\lambda_c - 2\mu)I_1 + (l + 2m)I_1^2 - 2m(I_1^2 + I_2)\right]\mathbf{I}$$
$$+ (2\mu + 2mI_1)\boldsymbol{\varepsilon} + n \cdot \mathrm{cof}(\boldsymbol{\varepsilon})$$
$$+ \left(2\gamma_2 I_1\zeta - \alpha M\zeta + \gamma_3\zeta^2\right)\mathbf{I},$$
$$\frac{\partial \Phi}{\partial \zeta} = -\alpha MI_1 + M\zeta + \gamma_2 I_1^2 + 2\gamma_3 I_1\zeta + 3\gamma_1\zeta^2, \tag{13}$$

where $\mathrm{cof}(\boldsymbol{\varepsilon})$ corresponds to the cofactor matrix of matrix $\boldsymbol{\varepsilon}$. Substituting Eqs. (5), (6), and (13) into Eq. (9), the equations of motion in terms of the displacements $\mathbf{u}$ and $\mathbf{w}$ are obtained as

$$\rho\ddot{\mathbf{u}} + \rho_f\ddot{\mathbf{w}} = \{[(\lambda_c - 2\mu)I_1 + (l + 2m)I_1^2 - 2m(I_2 - I_1^2)]\mathbf{F}$$
$$+ (2\mu + 2mI_1)\mathbf{F} \cdot \boldsymbol{\varepsilon} + n\mathbf{F} \cdot \mathrm{cof}(\boldsymbol{\varepsilon})$$
$$+ (2\gamma_2\zeta I_1 - \alpha M\zeta + \gamma_3\zeta^2)\mathbf{F}\} \cdot \overleftarrow{\nabla},$$
$$\rho_f + m' + \frac{\eta}{\kappa} = [(-\alpha MI_1 + M\zeta + \gamma_2 I_1^2$$
$$+ 2\gamma_3 I_1\zeta + 3\gamma_1\zeta^2)\mathbf{I}] \cdot \overleftarrow{\nabla} \tag{14}$$

Equation (14) is the governing equation for saturated porous materials based on the nonlinear cubic potential. This equation set is quite complex, it is difficult to study the property of nonlinearity. In order to investigate the nonlinear characteristics of porous materials, a one-dimensional wave equation will be further proposed in Sec. III.

III. ONE-DIMENSIONAL PROBLEM

A. One-dimensional governing equations

Although the general governing equations in a three-dimensional space are proposed and expressed in Eq. (14), the equation set is very complicated. Therefore, a simple

case, i.e., a plane wave propagating in one dimension, is selected to investigate the property of nonlinearity in saturated porous materials. On the basis of this assumption, the displacement for the solid component can be written as $\mathbf{u}(a,t) = (u_1, u_2, u_3)^T$, then the solid deformation gradient tensor is obtained as

$$\mathbf{F} = \begin{bmatrix} 1 + u_{1,a} & 0 & 0 \\ u_{2,a} & 1 & 0 \\ u_{3,a} & 0 & 1 \end{bmatrix}. \tag{15}$$

Substituting Eq. (15) into Eq. (2), the solid strain tensor is expressed as

$$\boldsymbol{\varepsilon} = \begin{bmatrix} u_{1,a} + \dfrac{1}{2}\mathbf{u}_{,a}{}^T \cdot \mathbf{u}_{,a} & \dfrac{1}{2}u_{2,a} & \dfrac{1}{2}u_{3,a} \\ \dfrac{1}{2}u_{2,a} & 0 & 0 \\ \dfrac{1}{2}u_{3,a} & 0 & 0 \end{bmatrix}. \tag{16}$$

Furthermore, the three invariants can also be obtained from the solid strain tensor

$$I_1 = \varepsilon_{11}, \quad I_2 = -(\varepsilon_{12}\varepsilon_{21} + \varepsilon_{13}\varepsilon_{31}), \quad I_3 = 0. \tag{17}$$

Substituting Eqs. (15), (16) and (17) into the first equation of Eq. (14), and then considering $\zeta = -\mathrm{div}\mathbf{w} = -w_{1,a}$, we have

$$\rho \ddot{u}_1 + \rho_f \ddot{w}_1 - (\lambda_c + 2\mu)\frac{\partial^2 u_1}{\partial a^2} - \alpha M \frac{\partial^2 w_1}{\partial a^2}$$
$$= \left\{ [3(\lambda_c + 2\mu) + 2(l + 2m)]\frac{\partial u_1}{\partial a}\frac{\partial^2 u_1}{\partial a^2} \right.$$
$$+ (\alpha M - 2\gamma_2)\left(\frac{\partial w_1}{\partial a}\frac{\partial^2 u_1}{\partial a^2} + \frac{\partial u_1}{\partial a}\frac{\partial^2 w_1}{\partial a^2}\right)$$
$$+ (\lambda_c + 2\mu + m)\left(\frac{\partial u_2}{\partial a}\frac{\partial^2 u_2}{\partial a^2} + \frac{\partial u_3}{\partial a}\frac{\partial^2 u_3}{\partial a^2}\right)$$
$$+ \left. 2\gamma_3 \frac{\partial w_1}{\partial a}\frac{\partial^2 w_1}{\partial a^2} \right\},$$
$$\rho \ddot{u}_2 + \rho_f \ddot{w}_2 - \mu \frac{\partial^2 u_2}{\partial a^2}$$
$$= (\lambda_c + 2\mu + m)\left(\frac{\partial u_1}{\partial a}\frac{\partial^2 u_2}{\partial a^2} + \frac{\partial u_2}{\partial a}\frac{\partial^2 u_1}{\partial a^2}\right),$$
$$\rho \ddot{u}_3 + \rho_f \ddot{w}_3 - \mu \frac{\partial^2 u_3}{\partial a^2}$$
$$= (\lambda_c + 2\mu + m)\left(\frac{\partial u_1}{\partial a}\frac{\partial^2 u_3}{\partial a^2} + \frac{\partial u_3}{\partial a}\frac{\partial^2 u_1}{\partial a^2}\right). \tag{18}$$

Note that the nonlinear terms are only retained to the third-order term and the higher order terms are omitted in Eq. (18). The same manipulation is performed on the second equation of Eq. (14), and another set of the governing equations can be obtained as

$$\rho_f \ddot{u}_1 + m' \ddot{w}_1 + \frac{\eta}{\kappa}\dot{w}_1 - \alpha M \frac{\partial^2 u_1}{\partial a^2} - M \frac{\partial^2 w_1}{\partial a^2}$$
$$= \left\{ (\alpha M - 2\gamma_2)\frac{\partial u_1}{\partial a}\frac{\partial^2 u_1}{\partial a^2} \right.$$
$$- \alpha M \left(\frac{\partial u_2}{\partial a}\frac{\partial^2 u_2}{\partial a^2} + \frac{\partial u_3}{\partial a}\frac{\partial^2 u_3}{\partial a^2}\right)$$
$$+ 2\gamma_3 \left(\frac{\partial w_1}{\partial a}\frac{\partial^2 u_1}{\partial a^2} + \frac{\partial u_1}{\partial a}\frac{\partial^2 w_1}{\partial a^2}\right)$$
$$- \left. 6\gamma_1 \frac{\partial w_1}{\partial a}\frac{\partial^2 w_1}{\partial a^2} \right\},$$
$$\rho_f \ddot{u}_2 + m' \ddot{w}_2 + \frac{\eta}{\kappa}\dot{w}_2 = 0,$$
$$\rho_f \ddot{u}_3 + m' \ddot{w}_3 + \frac{\eta}{\kappa}\dot{w}_3 = 0. \tag{19}$$

Similarly, the nonlinear terms in Eq. (19) are also retained up to the third-order. Equations (18) and (19) give the coupled one-dimensional wave equations propagating in saturated porous materials.

B. Nonlinear fields generated by one-dimensional longitudinal wave

Initially, only a longitudinal wave is considered for the one-dimensional problem, i.e., $u_2(a,t) = u_3(a,t) = 0$ and $w_2(a,t) = w_3(a,t) = 0$, then Eqs. (18) and (19) can be further simplified to

$$\rho \ddot{u}_1 + \rho_f \ddot{w}_1 - (\lambda_c + 2\mu)\frac{\partial^2 u_1}{\partial a^2} - \alpha M \frac{\partial^2 w_1}{\partial a^2}$$
$$= \left\{ [3(\lambda_c + 2\mu) + 2(l + 2m)]\frac{\partial u_1}{\partial a}\frac{\partial^2 u_1}{\partial a^2} \right.$$
$$+ (\alpha M - 2\gamma_2)\left(\frac{\partial w_1}{\partial a}\frac{\partial^2 u_1}{\partial a^2} + \frac{\partial u_1}{\partial a}\frac{\partial^2 w_1}{\partial a^2}\right)$$
$$+ \left. 2\gamma_3 \frac{\partial w_1}{\partial a}\frac{\partial^2 w_1}{\partial a^2} \right\},$$
$$\rho_f \ddot{u}_1 + m' \ddot{w}_1 + \frac{\eta}{\kappa}\dot{w}_1 - \alpha M \frac{\partial^2 u_1}{\partial a^2} - M \frac{\partial^2 w_1}{\partial a^2}$$
$$= \left\{ (\alpha M - 2\gamma_2)\frac{\partial u_1}{\partial a}\frac{\partial^2 u_1}{\partial a^2} \right.$$
$$+ 2\gamma_3 \left(\frac{\partial w_1}{\partial a}\frac{\partial^2 u_1}{\partial a^2} + \frac{\partial u_1}{\partial a}\frac{\partial^2 w_1}{\partial a^2}\right)$$
$$- \left. 6\gamma_1 \frac{\partial w_1}{\partial a}\frac{\partial^2 w_1}{\partial a^2} \right\}. \tag{20}$$

If the nonlinear terms in Eq. (20) are not considered, the coupled linear wave equations are recovered. To solve Eq. (20), the perturbation method is employed. The solutions are assumed as $u_1 = u_1^{(0)} + u_1^{(1)} + o(u_1^{(1)})$ and $w_1 = w_1^{(0)} + w_1^{(1)} + o(w_1^{(1)})$ with $u_1^{(0)} \gg u_1^{(1)}$ and $w_1^{(0)} \gg w_1^{(1)}$, and the higher order terms $o(*)$ can be omitted without causing large errors. Then, a set of linear coupled equations in terms of $u_1^{(0)}$ and $w_1^{(0)}$ can be obtained as

$$\rho \ddot{u}_1^{(0)} + \rho_f \ddot{w}_1^{(0)} - (\lambda_c + 2\mu)\frac{\partial^2 u_1^{(0)}}{\partial a^2} - \alpha M \frac{\partial^2 w_1^{(0)}}{\partial a^2} = 0,$$
$$\rho_f \ddot{u}_1^{(0)} + m' \ddot{w}_1^{(0)} + \frac{\eta}{\kappa}\dot{w}_1^{(0)} - \alpha M \frac{\partial^2 u_1^{(0)}}{\partial a^2} - M \frac{\partial^2 w_1^{(0)}}{\partial a^2} = 0. \tag{21}$$

In fact, Eq. (21) was proposed by Biot in his linear theory (Biot, 1962). Substituting u_1 and w_1 into the right hand side of Eq. (20), another nonlinear coupled equation can be derived in terms of $u_1^{(1)}$ and $w_1^{(1)}$ as follows:

$$\rho\ddot{u}_1^{(1)} + \rho_f\ddot{w}_1^{(1)} - (\lambda_c + 2\mu)\frac{\partial^2 u_1^{(1)}}{\partial a^2} - \alpha M\frac{\partial^2 w_1^{(1)}}{\partial a^2} = \left\{ \left[3(\lambda_c + 2\mu) + 2(l + 2m)\right]\frac{\partial u_1^{(0)}}{\partial a}\frac{\partial^2 u_1^{(0)}}{\partial a^2} \right.$$

$$+ (\alpha M - 2\gamma_2)\left(\frac{\partial w_1^{(0)}}{\partial a}\frac{\partial^2 u_1^{(0)}}{\partial a^2} + \frac{\partial u_1^{(0)}}{\partial a}\frac{\partial^2 w_1^{(0)}}{\partial a^2}\right)$$

$$\left. + 2\gamma_3\frac{\partial w_1^{(0)}}{\partial a}\frac{\partial^2 w_1^{(0)}}{\partial a^2} \right\},$$

$$\rho_f\ddot{u}_1^{(1)} + m'\ddot{w}_1^{(1)} + \frac{\eta}{\kappa}\dot{w}_1^{(1)} - \alpha M\frac{\partial^2 u_1^{(1)}}{\partial a^2} - M\frac{\partial^2 w_1^{(1)}}{\partial a^2} = \left\{ (\alpha M - 2\gamma_2)\frac{\partial u_1^{(0)}}{\partial a}\frac{\partial^2 u_1^{(0)}}{\partial a^2} \right.$$

$$+ 2\gamma_3\left(\frac{\partial w_1^{(0)}}{\partial a}\frac{\partial^2 u_1^{(0)}}{\partial a^2} + \frac{\partial u_1^{(0)}}{\partial a}\frac{\partial^2 w_1^{(0)}}{\partial a^2}\right)$$

$$\left. - 6\gamma_1\frac{\partial w_1^{(0)}}{\partial a}\frac{\partial^2 w_1^{(0)}}{\partial a^2} \right\}. \tag{22}$$

In Eq. (22), the higher order terms [e.g., $(\partial u_1^{(0)}/\partial a)(\partial^2 u_1^{(1)}/\partial a^2)$, $(\partial u_1^{(1)}/\partial a)(\partial^2 u_1^{(1)}/\partial a^2)$] are omitted. It is found that the nonlinear displacement fields $u_1^{(1)}$ and $w_1^{(1)}$ are generated by the linear displacement fields $u_1^{(0)}$ and $w_1^{(0)}$. In other words, the linear displacement fields can be regarded as the source of the nonlinear displacement fields. The solutions of Eq. (21) are expressed as follows (refer to the Appendix)

$$u_{1F}^{(0)}(a,t) = A_0 e^{j(k_F a - \omega t)}, \quad u_{1L}^{(0)}(a,t) = R_{BA} A_0 e^{j(k_L a - \omega t)},$$

$$w_{1F}^{(0)}(a,t) = \lambda_F A_0 e^{j(k_F a - \omega t)}, \quad w_{1L}^{(0)}(a,t) = R_{BA}\lambda_L A_0 e^{j(k_L a - \omega t)}, \tag{23}$$

where the subscripts "F" and "L" denote the fast wave and the slow wave, respectively, A_0 is the displacement amplitude of the fast wave at a source point, R_{BA} is the displacement amplitude ratio of the fast wave to the slow wave, k_i ($i = F, L$) is the wave number, ω is the angular frequency, and λ_i ($i = F, L$) is the amplitude ratio of w_i to u_i. If the wave field is stable, then the total displacement fields at a reference point are $u_1 = u_{1F}^{(0)} + u_{1L}^{(0)} + u_1^{(1)} + o(u_1^{(1)})$ and $w_1 = w_{1F}^{(0)} + w_{1L}^{(0)} + w_1^{(1)} + o(w_1^{(1)})$. Substituting these two expressions into Eq. (22), we have

$$\rho\ddot{u}_1^{(1)} + \rho_f\ddot{w}_1^{(1)} - (\lambda_c + 2\mu)\frac{\partial^2 u_1^{(1)}}{\partial a^2} - \alpha M\frac{\partial^2 w_1^{(1)}}{\partial a^2}$$

$$= \left\{ -jA_0^2\left\{\left[3(\lambda_c + 2\mu) + 2(l + 2m) + 2(\alpha M - 2\gamma_2)\lambda_F + 2\gamma_3\lambda_F^2\right]\right\}k_F^3 e^{j(2k_F a)} \right.$$

$$-jA_0^2\left\{\left[3(\lambda_c + 2\mu) + 2(l + 2m) + (\alpha M - 2\gamma_2)(\lambda_F + \lambda_L) + 2\gamma_3\lambda_F\lambda_L\right]\right\}(k_F^2 k_L + k_L^2 k_F)R_{BA} e^{j(k_F + k_L)a}$$

$$\left. -jA_0^2\left\{\left[3(\lambda_c + 2\mu) + 2(l + 2m) + 2(\alpha M - 2\gamma_2)\lambda_L + 2\gamma_3\lambda_L^2\right]\right\}k_L^3 R_{BA}^2 e^{j(2k_L a)} \right\}e^{-j2\omega t},$$

$$\rho_f\ddot{u}_1^{(1)} + m'\ddot{w}_1^{(1)} + \frac{\eta}{\kappa}\dot{w}_1^{(1)} - \alpha M\frac{\partial^2 u_1^{(1)}}{\partial a^2} - M\frac{\partial^2 w_1^{(1)}}{\partial a^2}$$

$$= \left\{ -jA_0^2\left[(\alpha M - 2\gamma_2) + 4\gamma_3\lambda_F - 6\gamma_1\lambda_F^2\right]k_F^3 e^{j(2k_F a)} \right.$$

$$-jA_0^2\left[(\alpha M - 2\gamma_2) + 2\gamma_3(\lambda_F + \lambda_L) - 6\gamma_1\lambda_F\lambda_L\right](k_F^2 k_L + k_L^2 k_F)R_{BA} e^{j(k_F + k_L)a}$$

$$\left. -jA_0^2\left[(\alpha M - 2\gamma_2) + 4\gamma_3\lambda_L - 6\gamma_1\lambda_L^2\right]k_L^3 R_{BA}^2 e^{j(2k_L a)} \right\}e^{-j2\omega t}. \tag{24}$$

In Eq. (24), it is clear that the vibration frequency of the nonlinear displacement is double of the linear displacement. Therefore, a longitudinal wave with a frequency ω can generate a double-frequency longitudinal wave in an unbounded medium due to the nonlinear property. It is assumed that the solutions to Eq. (24) are $u_1^{(1)} = \bar{u}_1^{(1)}e^{-j2\omega t}$ and $w_1^{(1)} = \bar{w}_1^{(1)}e^{-j2\omega t}$. For brevity, $\bar{u}_1^{(1)}$ and $\bar{w}_1^{(1)}$ are, respectively, simplified as $u^{(1)}$ and $w^{(1)}$ in the following. Substituting the two solutions into Eq. (24), we obtain

$$-(\lambda_c + 2\mu)\frac{\partial^2 u^{(1)}}{\partial a^2} - \alpha M\frac{\partial^2 w^{(1)}}{\partial a^2} - \rho(2\omega)^2 u^{(1)} - \rho_f(2\omega)^2 w^{(1)} = G_1,$$

$$-\alpha M\frac{\partial^2 u^{(1)}}{\partial a^2} - M\frac{\partial^2 w^{(1)}}{\partial a^2} - \rho_f(2\omega)^2 u^{(1)} - m'(2\omega)^2 w^{(1)} - j(2\omega)\frac{\eta}{\kappa}w^{(1)} = G_2, \tag{25}$$

where $G_1 = G_{11} + G_{12} + G_{13}$ and $G_2 = G_{21} + G_{22} + G_{23}$, in which

$$G_{11} = -jA_0{}^2 B_{11} k_F{}^3 e^{j(2k_F a)},$$

$$G_{12} = -jA_0{}^2 B_{12}(k_F{}^2 k_L + k_L{}^2 k_F) e^{j(k_F+k_L)a},$$

$$G_{13} = -jA_0{}^2 B_{13} k_L{}^3 e^{j(2k_L a)},$$

$$G_{21} = -jA_0{}^2 B_{21} k_F{}^3 e^{j(2k_F a)},$$

$$G_{22} = -jA_0{}^2 B_{22}(k_F{}^2 k_L + k_L{}^2 k_F) e^{j(k_F+k_L)a},$$

$$G_{23} = -jA_0{}^2 B_{23} k_L{}^3 e^{j(2k_L a)},$$

$$B_{11} = 3(\lambda_c + 2\mu) + 2(l + 2m)$$
$$+ 2(\alpha M - 2\gamma_2)\lambda_F + 2\gamma_3 \lambda_F{}^2,$$

$$B_{12} = R_{BA}[3(\lambda_c + 2\mu) + 2(l + 2m)$$
$$+ (\alpha M - 2\gamma_2)(\lambda_F + \lambda_L) + 2\gamma_3 \lambda_F \lambda_L],$$

$$B_{13} = R_{BA}{}^2[3(\lambda_c + 2\mu) + 2(l + 2m)$$
$$+ 2(\alpha M - 2\gamma_2)\lambda_L + 2\gamma_3 \lambda_L{}^2],$$

$$B_{21} = (\alpha M - 2\gamma_2) + 4\gamma_3 \lambda_F - 6\gamma_1 \lambda_F{}^2,$$

$$B_{22} = R_{BA}[(\alpha M - 2\gamma_2) + 2\gamma_3(\lambda_F + \lambda_L) - 6\gamma_1 \lambda_F \lambda_L],$$

$$B_{23} = R_{BA}{}^2[(\alpha M - 2\gamma_2) + 4\gamma_3 \lambda_L - 6\gamma_1 \lambda_L{}^2].$$

By eliminating $w^{(1)}$ from Eq. (25), a fourth-order nonhomogeneous differential equation is obtained as

$$c_4 \frac{\partial^4 u^{(1)}}{\partial a^4} + c_2 \frac{\partial^2 u^{(1)}}{\partial a^2} + c_0 u^{(1)}$$
$$= H_{NF} e^{j(2k_F a)} + H_{NM} e^{j(k_F+k_L)a} + H_{NL} e^{j(2k_L a)}, \quad (26)$$

where

$$c_4 = \alpha M \beta_1,$$

$$c_2 = (\lambda_c + 2\mu) + \alpha M \beta_2 + \rho_f (2\omega)^2 \beta_1,$$

$$c_0 = \rho_f (2\omega)^2 \beta_2 + \rho(2\omega)^2,$$

$$H_{NF} = -jA_0{}^2 \left\{ B_{11} + (B_{11} - \alpha B_{21}) \right.$$
$$\left. \times \left[\rho_f(2\omega)^2 \beta_3 - \alpha M \beta_3 (2k_F)^2 \right] k_F{}^3 \right\},$$

$$H_{NM} = -jA_0{}^2 \left\{ B_{12} + (B_{12} - \alpha B_{22}) \right.$$
$$\left. \times \left[\rho_f(2\omega)^2 \beta_3 - \alpha M \beta_3 (k_F + k_L)^2 \right] (k_F{}^2 k_L + k_L{}^2 k_F) \right\},$$

$$H_{NL} = -jA_0{}^2 \left\{ B_{13} + (B_{13} - \alpha B_{23}) \right.$$
$$\left. \times \left[\rho_f(2\omega)^2 \beta_3 - \alpha M \beta_3 (2k_L)^2 \right] k_L{}^3 \right\},$$

$$\beta_1 = -\frac{\alpha^2 M - (\lambda_c + 2\mu)}{\alpha m'(2\omega)^2 + j(2\omega)\frac{\alpha\eta}{\kappa} - \rho_f(2\omega)^2},$$

$$\beta_2 = -\frac{\alpha \rho_f(2\omega)^2 - \rho(2\omega)^2}{\alpha m'(2\omega)^2 + j(2\omega)\frac{\alpha\eta}{\kappa} - \rho_f(2\omega)^2},$$

$$\beta_3 = \frac{1}{\alpha m'(2\omega)^2 + j(2\omega)\frac{\alpha\eta}{\kappa} - \rho_f(2\omega)^2}.$$

Introducing two complex wave numbers k_{NF} and k_{NL} satisfies

$$k_{NF}{}^2 + k_{NL}{}^2 = \frac{c_2}{c_4}, \quad k_{NF}{}^2 \cdot k_{NL}{}^2 = \frac{c_0}{c_4},$$
$$\mathrm{Re}(k_{NL}) > \mathrm{Re}(k_{NF}) > 0. \quad (27)$$

Then, Eq. (26) can be rewritten as

$$\left(\frac{\partial^2}{\partial a^2} + k_{NF}{}^2 \right) \left(\frac{\partial^2}{\partial a^2} + k_{NL}{}^2 \right) u^{(1)}$$
$$= \frac{1}{a_0} \left[H_{NF} e^{j(2k_F a)} + H_{NM} e^{j(k_F+k_L)a} + H_{NL} e^{j(2k_L a)} \right]. \quad (28)$$

The nonlinear displacement field is generated by the interaction of the linear displacements. Consequently, the homogeneous solution of Eq. (26) disappears and only the nonhomogeneous solution exists. To solve Eq. (28), the dissipation characteristics of the system should be considered. For a non-dissipative system, the wave number keeps a linear dependence with the frequency, this implies $k_{Ni} = 2k_i$ ($i = F, L$). Hence, the particular solutions corresponding to the first and third terms on the right-hand side of Eq. (28) possess a cumulative effect along the distance. However, this relationship cannot hold for a dissipative system. It is well known that the attenuation of fast waves is small while the attenuation of slow waves is stronger. Therefore, the porous medium is considered as a non-dissipative system for the fast waves, while it is a dissipative system for the slow waves, as shown in Fig. 1. The material parameters are calculated using the relative parameters (Donskoy et al., 1997) (see Sec. IV A). From Fig. 1, we found that the imaginary part of the wave numbers is significantly small for the fast waves. Hence, the non-dissipative approximation for the fast waves is reasonable. The large imaginary part of the wave numbers indicates the dissipative property of the slow waves. Note that the non-dissipative characteristics were assumed to obtain the wave solutions for the fast and slow waves (Donskoy et al., 1997). Based on the above interpretation, replacing k_{NF} with $2k_F$, then the solution of Eq. (28) is obtained as

$$u_N{}^{(1)} = u_{NF}{}^{(1)} + u_{NM}{}^{(1)} + u_{NL}{}^{(1)}, \quad (29)$$

where

$$u_{NF}{}^{(1)} = \frac{H_{NF}}{c_4} \frac{-20k_F{}^2 + k_{NL}{}^2 + j16k_F{}^3 a - j4k_F k_{NL}{}^2 a}{16k_F{}^2(-4k_F{}^2 + k_{NL}{}^2)^2} e^{j2k_F a},$$

$$u_{NM}{}^{(1)} = \frac{H_{NM}}{c_4} \frac{1}{(k_F - k_L)(3k_F + k_L)\left[-k_{NL}{}^2 + (k_F + k_L)^2 \right]}$$
$$\times e^{j(k_F+k_L)a},$$

$$u_{NL}{}^{(1)} = \frac{H_{NL}}{c_4} \frac{1}{4(k_L{}^2 - k_F{}^2)(4k_L{}^2 - k_{NL}{}^2)} e^{j2k_L a}. \quad (30)$$

Combining Eq. (23) and Eq. (29), the total displacement for the solid is

$$u_1 = u_{1F}{}^{(0)} + u_{1L}{}^{(0)} + u_{NF}{}^{(1)} + u_{NM}{}^{(1)} + u_{NL}{}^{(1)}. \quad (31)$$

J. Acoust. Soc. Am. **142** (2), August 2017

Tong et al. 761
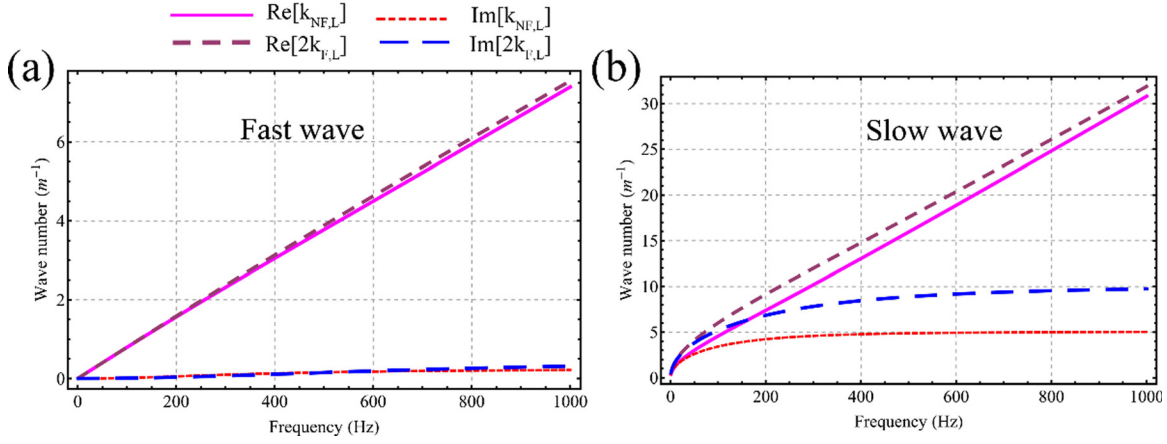
FIG. 1. (Color online) Comparison of the values of (a) k_{NF} and $2k_F$; and (b) k_{NL} and $2k_L$.

From Eq. (30), the nonlinear displacement fields contain three kinds of longitudinal waves. The first and third ones are generated by the fast wave and the slow wave, respectively. The second one is generated by the interaction of the fast and slow waves. It is interesting that there exists a new nonlinear wave with a wave velocity located between the fast wave speed and the slow wave speed.

C. Nonlinear longitudinal waves generated by shear wave

It is unlikely the one-dimensional longitudinal wave that can generate a double-frequency longitudinal wave within the nonlinear consideration, a one-dimensional shear wave with a frequency ω cannot generate a double frequency shear wave, while it can generate a longitudinal wave with a frequency 2ω, as shown in Eqs. (18) and (19). Assuming that $u_1^{(0)}(a, t) = u_3^{(0)}(a, t) = 0$ and $w_1^{(0)}(a, t) = w_3^{(0)}(a, t) = 0$, there is only one shear wave source in the medium. Denote the high order longitudinal displacements as $u_1^{(1)}$ and $w_1^{(1)}$, then Eqs. (18) and (19) become

$$\rho \ddot{u}_2^{(0)} + \rho_f \ddot{w}_2^{(0)} - \mu \frac{\partial^2 u_2^{(0)}}{\partial a^2} = 0,$$
$$\rho_f \ddot{u}_2^{(0)} + m' \ddot{w}_2^{(0)} + \frac{\eta}{\kappa} \dot{w}_2^{(0)} = 0 \qquad (32)$$

and

$$\rho \ddot{u}_1^{(1)} + \rho_f \ddot{w}_1^{(1)} - (\lambda_c + 2\mu) \frac{\partial^2 u_1^{(1)}}{\partial a^2} - \alpha M \frac{\partial^2 w_1^{(1)}}{\partial a^2}$$
$$= (\lambda_c + 2\mu + m) \frac{\partial u_2^{(0)}}{\partial a} \frac{\partial^2 u_2^{(0)}}{\partial a^2},$$
$$\rho_f \ddot{u}_1^{(1)} + m' \ddot{w}_1^{(1)} + \frac{\eta}{\kappa} \dot{w}_1^{(1)} - \alpha M \frac{\partial^2 u_1^{(1)}}{\partial a^2} - M \frac{\partial^2 w_1^{(1)}}{\partial a^2}$$
$$= -\alpha M \frac{\partial u_2^{(0)}}{\partial a} \frac{\partial^2 u_2^{(0)}}{\partial a^2}. \qquad (33)$$

Equation (32) is a coupled linear shear wave equation, while Eq. (33) is the governing equation for generating the high order longitudinal waves. If the frequency of the shear wave is ω and $u_2^{(0)} = \bar{u}_2^{(0)} e^{-j\omega t}$, we obtain

$$\mu \frac{\partial^2 \bar{u}_2^{(0)}}{\partial a^2} + \left(\rho \omega^2 - \frac{\rho_f^2 \omega^4}{j\omega \frac{\eta}{\kappa} + m'\omega^2} \right) \bar{u}_2^{(0)} = 0,$$
$$\bar{w}_2^{(0)} = \lambda_s \bar{u}_2^{(0)}, \qquad (34)$$

where $\lambda_s = -(\rho_f \omega^2)/[(j\omega\eta/\kappa) + m'\omega^2]$. Only the shear wave propagating in the positive direction is considered, then the solutions of Eq. (34) are

$$\bar{u}_2^{(0)} = A_s e^{jk_s a},$$
$$\bar{w}_2^{(0)} = \lambda_s A_s e^{jk_s a}, \qquad (35)$$

where A_s is the amplitude of the shear wave at the source point that can be determined by the boundary conditions, and $k_s = \sqrt{(\rho\omega^2 - [(\rho_f^2 \omega^4)/j\omega(\eta/\kappa) + m'\omega^2])/\mu}$ is the shear wave number. Substituting Eq. (35) into Eq. (33), the higher order longitudinal wave equations can be rewritten as

$$\rho \ddot{u}_1^{(1)} + \rho_f \ddot{w}_1^{(1)} - (\lambda_c + 2\mu) \frac{\partial^2 u_1^{(1)}}{\partial a^2} - \alpha M \frac{\partial^2 w_1^{(1)}}{\partial a^2}$$
$$= -jA_s^2 k_s^3 (\lambda_c + 2\mu + m) e^{j(2k_s a - 2\omega t)},$$
$$\rho_f \ddot{u}_1^{(1)} + m' \ddot{w}_1^{(1)} + \frac{\eta}{\kappa} \dot{w}_1^{(1)} - \alpha M \frac{\partial^2 u_1^{(1)}}{\partial a^2} - M \frac{\partial^2 w_1^{(1)}}{\partial a^2}$$
$$= -jA_s^2 k_s^3 \alpha M e^{j(2k_s a - 2\omega t)}. \qquad (36)$$

As there is no longitudinal wave source, the time dependent term $e^{-j\omega t}$ disappears in the solutions. Making use of $u_1^{(1)} = \bar{u}_1^{(1)} e^{-j2\omega t}$ and $w_1^{(1)} = \bar{w}_1^{(1)} e^{-j2\omega t}$, then a fourth-order differential equation is obtained from Eq. (36) as

$$c_4 \frac{\partial^4 \bar{u}_1^{(1)}}{\partial a^4} + c_2 \frac{\partial^2 \bar{u}_1^{(1)}}{\partial a^2} + c_0 \bar{u}_1^{(1)} = H_s e^{j(2k_s a)}, \qquad (37)$$

where $H_s = jA_s^2 [\lambda_c + 2\mu + m - \alpha M \beta_1 (2k_s)^2 + \rho_f (2\omega)^2 \beta_1] k_s^3$. The parameters c_4, c_2, c_0, and β_1 are defined in Eq. (26). Considering no reflection condition in an infinite medium, the solution of Eq. (37) can be expressed as

$$u_1^{(1)} = u_{1h}^{(1)} + u_{1p}^{(1)}, \tag{38}$$

where

$$u_{1h}^{(1)} = \underbrace{A_{NF} e^{j(k_{NF}a - 2\omega t)}}_{u_{NF}} + \underbrace{A_{NL} e^{j(k_{NL}a - 2\omega t)}}_{u_{NL}},$$

$$u_{1p}^{(1)} = \underbrace{\frac{H_s}{c_0 - 4c_2 k_s{}^2 + 16c_4 k_s{}^4} e^{j(2k_s a - 2\omega t)}}_{u_{NP}}. \tag{39}$$

The wave numbers k_{NF} and k_{NL} in Eq. (39) also satisfy Eq. (27). The parameters A_{NF} and A_{NL} in Eq. (39) are constants that can be determined by the boundary conditions. From Eq. (36), we also obtain

$$w_1^{(1)} = \beta_1 \frac{\partial^2 u_1^{(1)}}{\partial a^2} + \beta_2 u_1^{(1)} - j\beta_6 A_s{}^2 k_s{}^3 e^{j2k_s a}, \tag{40}$$

where $\beta_6 = -\{[\alpha^2 M - (\lambda_c + 2\mu + m)]/[\alpha\ m'(2\omega)^2 + j(2\omega)(\alpha\eta/\kappa) - \rho_f(2\omega)^2]\}$. As the nonlinear displacement field is generated by a shear wave, thus we have the following boundary conditions:

$$u_1^{(1)}(0, t) = 0,$$
$$w_1^{(1)}(0, t) = 0. \tag{41}$$

Combining Eqs. (38), (40), and (41), the constants A_{NF} and A_{NL} are then solved as

$$A_{NF} = \frac{j\beta_6 A_s{}^2 k_s{}^3 - \beta_1 \left[k_{NL}{}^2 - (2k_s)^2\right] Q_s}{\beta_1 (k_{NL}{}^2 - k_{NF}{}^2)},$$

$$A_{NL} = \frac{j\beta_6 A_s{}^2 k_s{}^3 - \beta_1 \left[k_{NF}{}^2 - (2k_s)^2\right] Q_s}{\beta_1 (k_{NF}{}^2 - k_{NL}{}^2)}, \tag{42}$$

where $Q_s = [H_s/(c_0 - 4c_2 k_s{}^2 + 16c_4 k_s{}^4)]$. From the above mathematical derivation, only a double-frequency nonlinear longitudinal wave is generated under the condition of a single one-dimensional shear wave source. From Eq. (38), it is found that there are three nonlinear waves propagating in the medium with the wave speeds $2\omega/\mathrm{Re}(k_{NF})$, $2\omega/\mathrm{Re}(k_{NL})$, and $\omega/\mathrm{Re}(k_s)$, which correspond to the waves u_{NF}, u_{NL}, and u_{NP}, respectively. Obviously, the nonlinear wave u_{NP} has the same wave speed as the shear wave. As $\mathrm{Re}(k_{NL}) > \mathrm{Re}(k_{NF})$, the wave speed of u_{NF} is larger than that of u_{NL}. As a result, the waves u_{NF} and u_{NL} can be called as the fast nonlinear wave and the slow nonlinear wave, respectively. Through the numerical analysis, the slow nonlinear wave shows the same attenuation property to that of the linear slow wave. Hence, it can only propagate within short distances. It is interesting that a fast nonlinear wave can be observed even before the arrival of a shear wave, because the speed of the fast nonlinear wave is greatly faster than that of the shear wave. On the basis of the experimental observation (Bouzidi and Schmitt, 2009), an unsuspected wave appears before the arrival of a shear wave. They attributed this phenomenon to the transducer edge effect. We infer that the unsuspected

wave is probably the nonlinear fast wave generated by a shear wave. If the one-dimensional longitudinal and shear wave sources are coherently applied in porous materials, then both the double-frequency longitudinal and shear waves will be generated due to the nonlinear interaction. The corresponding derivation can be easily carried out by referring the aforementioned discussion.

In this paper, only the explicit nonlinear displacement fields for solid components are presented in the aforementioned works. However, the nonlinear displacement fields for fluid components can be obtained from Eq. (25) or Eq. (36) for a one-dimensional longitudinal wave problem or a one-dimensional shear wave problem, respectively. Hence, it is not presented herein.

D. Determination of nonlinear parameters γ_1, γ_2, and γ_3

As there are no measurements attempted on the nonlinear elastic constants γ_1, γ_2, and γ_3, we determine these parameters by some special cases. If the porous medium degenerates to a single phase liquid (i.e., the porosity equals to unity), then the strain energy immediately becomes

$$\Phi = \frac{1}{2} M \zeta^2 + \gamma_1 \zeta^3. \tag{43}$$

According to the definition of the parameter M (Biot, 1962), $M = 1/c$ for $n_0 = 1$ with c the fluid compressibility. Besides, we also found that $\zeta = -\mathrm{div}\mathbf{U} = \delta_f$ for $n_0 = 1$ in which $\delta_f = \Delta\rho_f/\rho_f$. Substituting M and ζ into Eq. (43) yields

$$\Phi = \frac{1}{2c} \delta_f{}^2 + \gamma_1 \delta_f{}^3. \tag{44}$$

Then, the fluid pressure can be readily derived as

$$p_f = \frac{\partial\Phi}{\partial\delta_f} = \frac{\delta_f}{c} + 3\gamma_1 \delta_f{}^2. \tag{45}$$

By comparing with the liquid pressure in the work of Zhu et al. (1983), the nonlinear parameter γ_1 can be determined as

$$\gamma_1 = \frac{1}{6c} \beta_f, \tag{46}$$

in which β_f is the fluid nonlinearity parameter denoted by B/A (Zhu et al., 1983). In most liquid media, the value of β_f ranges from 5 to 10 (Zhu et al., 1983). Hence, the value of the nonlinear parameter γ_1 is on the same order of $1/c$.

To determine the nonlinear parameter γ_3, the solid component of the porous medium is restricted to be rigid, thus the solid displacement is $\mathbf{u} = \mathbf{0}$. For a one-dimensional problem, the coupled Eq. (22) reduces to

$$\rho_f \ddot{w}_1^{(1)} - \alpha M \frac{\partial^2 w_1^{(1)}}{\partial a^2} = 2\gamma_3 \frac{\partial w_1^{(0)}}{\partial a} \frac{\partial^2 w_1^{(0)}}{\partial a^2},$$

$$m' \ddot{w}_1^{(1)} + \frac{\eta}{\kappa} \dot{w}_1^{(1)} - M \frac{\partial^2 w_1^{(1)}}{\partial a^2} = -6\gamma_1 \frac{\partial w_1^{(0)}}{\partial a} \frac{\partial^2 w_1^{(0)}}{\partial a^2}. \tag{47}$$

J. Acoust. Soc. Am. **142** (2), August 2017

Tong *et al.* 763

Assume the first-order nonlinear liquid displacement $w_1^{(1)} = A_1 e^{j\omega[(a/C_L)-t]}$ and substitute it into Eq. (47) to obtain

$$\gamma_3 = -3\gamma_1 \frac{\alpha M - \rho_f C_L^2}{M - m'C_L^2 - j\frac{\eta}{2\kappa}\frac{C_L^2}{\omega}}, \qquad (48)$$

in which C_L is the wave speed of a porous medium with a rigid solid component. Under the assumption of a rigid solid, the fast wave speed tends to infinity. As a result, C_L corresponds to the slow wave speed with the expression of $C_L = \omega/k_L$. Note that γ_3 in Eq. (48) is a complex value that violates a physical conception. For a better estimation, the real part of Eq. (48) is selected as the final value of γ_3.

When the "*dynamic compatibility*" relationship expressed in Biot's work (Biot, 1956a) is satisfied, there is no relative motion between fluid and solid bodies, i.e., $\mathbf{w} = \mathbf{0}$. Under this condition, for a one-dimensional problem, Eq. (22) reduces to

$$\rho \ddot{u}_1^{(1)} - (\lambda_c + 2\mu)\frac{\partial^2 u_1^{(1)}}{\partial a^2} = \left[3(\lambda_c + 2\mu) + 2(l + 2m)\right]$$
$$\times \frac{\partial u_1^{(0)}}{\partial a}\frac{\partial^2 u_1^{(0)}}{\partial a^2},$$
$$\rho_f \ddot{u}_1^{(1)} - \alpha M\frac{\partial^2 u_1^{(1)}}{\partial a^2} = (\alpha M - 2\gamma_2)\frac{\partial u_1^{(0)}}{\partial a}\frac{\partial^2 u_1^{(0)}}{\partial a^2}.$$
$$(49)$$

Assume the first-order nonlinear liquid displacement $u_1^{(1)} = A_2 e^{j\omega[(a/C_F)-t]}$ and substitute it into Eq. (49) to obtain

$$\gamma_2 = \frac{\alpha M}{2} - \frac{1}{2}\frac{\alpha M - \rho_f C_F^2}{(\lambda_c + 2\mu) - \rho C_F^2}\left[3(\lambda_c + 2\mu) + 2(l + 2m)\right], \qquad (50)$$

where C_F is the wave speed of a solid component of the porous medium. Typically, the wave speed is faster in solids than in liquids, thus C_F is taken as the fast wave speed, i.e.,

$C_F = \omega/k_F$. For physical reasonableness, the real part of Eq. (50) is taken as the final value of the nonlinear parameter γ_2. From the experimental observation (Porubov and Maugin, 2009), the presence of pores significantly enhances the nonlinearity of porous materials to make $l, m \gg \lambda, M, \mu$. As a result, the value of γ_2 in Eq. (50) is on the order of l and m.

IV. RESULTS AND DISCUSSION

A. Nonlinear displacements generated by one-dimensional longitudinal wave

To investigate the nonlinear displacement fields generated by a one-dimensional longitudinal wave source, we consider a practical water-saturated sandy sediment (Donskoy *et al.*, 1997) with the physical parameters $\rho_s = 2650\,\mathrm{kg\,m^{-3}}$, $\rho_f = 1000\,\mathrm{kg\,m^{-3}}$, $M = 4.57\,\mathrm{GPa}$, $\lambda_c = 4.62\,\mathrm{GPa}$, $\alpha = 0.994$, $\mu = 0.167\,\mathrm{GPa}$, and $n_0 = 0.4$. The permeability coefficient was not given in the work of Donskoy *et al.* (1997), where a non-dissipative system was assumed. In a study of a similar material by Lee *et al.* (2007), the permeability $\kappa = 1 \times 10^{-10}\,\mathrm{m^{-2}}$ and the dynamic viscosity of water $\eta = 0.001\,\mathrm{Pa\,s}$ were used. Assuming that the fluid compressibility $c = 0.44\,\mathrm{GPa^{-1}}$ and $\beta_f = 5.11$ for water at a normal temperature (Zhu *et al.*, 1983), the nonlinear parameter γ_1 can be calculated as $\gamma_1 = 1.93\,\mathrm{GPa}$. From the work of Porubov and Maugin (2009), the nonlinear parameters l and m of a porous medium range from $10^3\,\mathrm{GPa}$ to $10^4\,\mathrm{GPa}$. Because the effective nonlinear parameter Γ is estimated as 1300 when the porosity $n_0 = 0.4$(Donskoy *et al.*, 1997), we use $l = m = -10^3(\lambda_c + 2\mu)$ for the subsequent investigation. Besides, no measurements of coupled nonlinear elastic constants have been reported, we resort to Eqs. (48) and (50) proposed in Sec. III. The practical situation considered here is described in the Appendix, wherein R_{BA} is approximated using Eq. (A14) for the following simulation. The parameters used for the following analysis are also listed in Table I.

TABLE I. Parameters of solid, fluid and porous frames.

Parameter	Definition	Value	Unit	Remark
ρ_s	Density of solid	2650	kg/m³	Donskoy *et al.* (1997)
ρ_f	Density of fluid	1000	kg/m³	Donskoy *et al.* (1997)
ρ	Density of the bulk material	1990	kg/m³	$n_0\rho_f + (1 - n_0)\rho_s$
K_b	Frame bulk modulus	0.211	GPa	$= \lambda + 2\mu/3$
K_s	Frame unjacketed bulk modulus	36	GPa	Assumed = Solid bulk modulus (Bouzidi and Schmitt, 2009)
α	Biot parameter	0.994	dimensionless	$\approx 1 - K_b/K_s$ (Tong *et al.*, 2016)
M	Biot parameter	4.57	GPa	Biot (1962)
λ	Lame coefficients	0.1	GPa	Selected in this work
μ	Lame coefficients	0.167	GPa	Selected in this work
κ	Permeability coefficient	10^{-10}	m⁻²	Lee *et al.* (2007)
η	Dynamic viscosity	0.001	Pa s	Lee *et al.* (2007)
n_0	Porosity	0.4	dimensionless	Donskoy *et al.* (1997)
β_f	Fluid nonlinearity parameter	5.11	dimensionless	Zhu *et al.* (1983)
c	Fluid compressibility	0.44	GPa⁻¹	Zhu *et al.* (1983)
l	Nonlinear elastic constants	−4.95	TPa	Estimated in this work
m	Nonlinear elastic constants	−4.95	TPa	Estimated in this work
γ_1	Nonlinear elastic constants	1.93	GPa	Eq. (46)
γ_3	Coupled Nonlinear elastic constants	−5.9	GPa	At 100 Hz, Eq. (48)
γ_2	Coupled Nonlinear elastic constants	−25.6	TPa	At 100 Hz, Eq. (50)
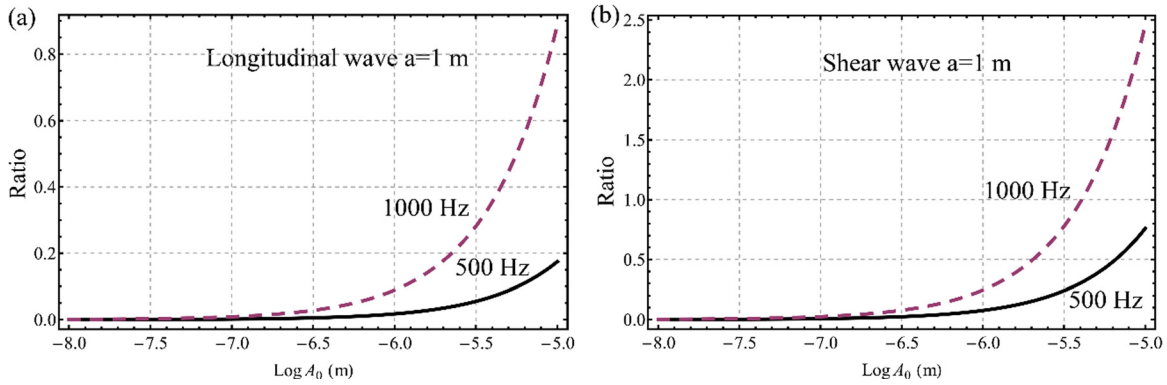
FIG. 2. (Color online) Ratio of the nonlinear displacement amplitudes versus the linear displacement amplitudes for different frequencies. (a) The nonlinear wave generated by a longitudinal wave at $a = 1$ m; and (b) the nonlinear wave generated by a shear wave at $a = 1$ m. The "longitudinal wave" and "shear wave" in the figures indicate the nonlinear displacement fields generated by the longitudinal and shear waves, respectively.

Figure 2 shows the ratio of the nonlinear displacement amplitudes generated by a one-dimensional longitudinal wave and a shear wave to the corresponding linear displacement amplitudes. When the linear displacement amplitude at the source point A_0 exceeds 0.3 μm, the nonlinear displacement becomes more significant and cannot be omitted. Numerical analysis indicates that the major contribution to the nonlinear displacement comes from the slow wave acting across a short distance. The slow wave length is around 0.4 m at a frequency of 1000 Hz, and the corresponding strain amplitude is about 4.2×10^{-5}. This is consistent with the experimental observation of Johnson and Jia (2005). In the following discussion, the linear displacement amplitude of fast waves at the source is chosen as $A_0 = 10^{-6}$ m. Note that the modulus of porous materials is experimentally known to be a function of the strain amplitude (Johnson and Jia, 2005). However, the variation of the modulus is negligible (less than 6%). Therefore, the linear elastic parameters are assumed to be constant for the subsequent discussion.

To illustrate the importance of the coupled nonlinear parameters γ_2 and γ_3, Fig. 3 shows the nonlinear displacements generated by a one-dimensional longitudinal wave when using the proposed values of those parameters, compared with the case in which $\gamma_2 = 0$ and $\gamma_3 = 0$. Clearly, the presence of the non-zero coupled nonlinear parameters γ_2 and γ_3 significantly increases the total nonlinear displacement. For

the frequency response at 100 Hz, the presence of γ_2 and γ_3 raises the nonlinear displacement by about 5 dB at the far distance, by more than 10 dB at a distance less than 1.2 m, and by about 15 dB at a distance of 1 m. Therefore, in the absence of the solid-fluid coupling nonlinear parameters γ_2 and γ_3, the total nonlinear displacement would be under-estimated, leading to an error.

Figure 4 shows the variation of the displacement levels of the solid components at different frequencies. The linear displacement, that is, the summation of the displacements of linear fast and slow waves, is also presented as a reference. The nonlinear displacement is calculated by Eq. (29). The linear displacement amplitude is slightly attenuated in the near field and remains nearly constant in the far field at the frequencies of both 100 Hz and 1000 Hz. However, the nonlinear displacement is sharply attenuated below the distance a <1.9 m for 100 Hz, while a <1 m for 1000 Hz. This displacement remains constant beyond distances of 3.2 m for 100 Hz and 1.5 m for 1000 Hz. It is also interesting that the amplitudes appear at distances ranging from 1.9 m to 3.2 m at 100 Hz and 1.1 m to 1.5 m at 1000 Hz. The minima are attributed to the interference of the three nonlinear waves due to the phase difference between them.

From Fig. 5, it is clear that the three particular solutions of Eq. (30) respond differently to changes of distance. For the 100 Hz frequency response, the nonlinear displacement
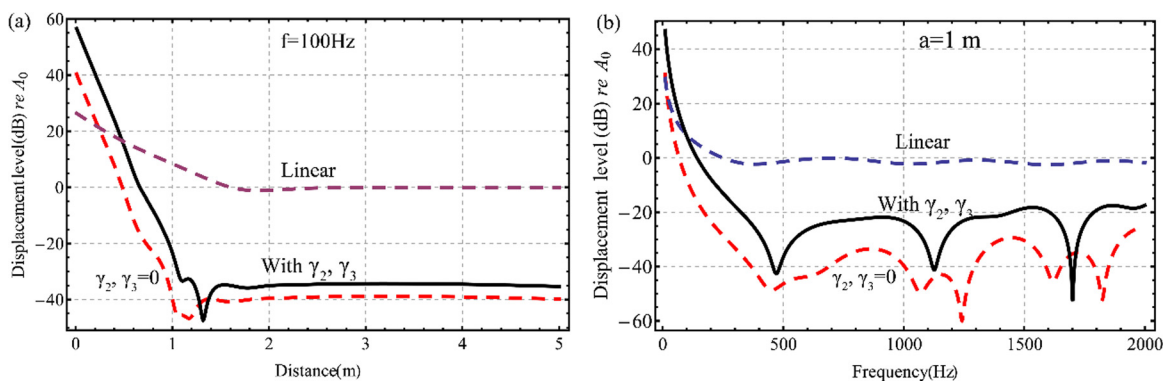
FIG. 3. (Color online) Comparison of the nonlinear displacements generated by a one-dimensional longitudinal wave with and without γ_2 and γ_3. (a) Displacement level versus distance; and (b) Displacement level versus frequency. The vertical axis is the ratio of the linear and nonlinear displacement amplitudes to A_0.
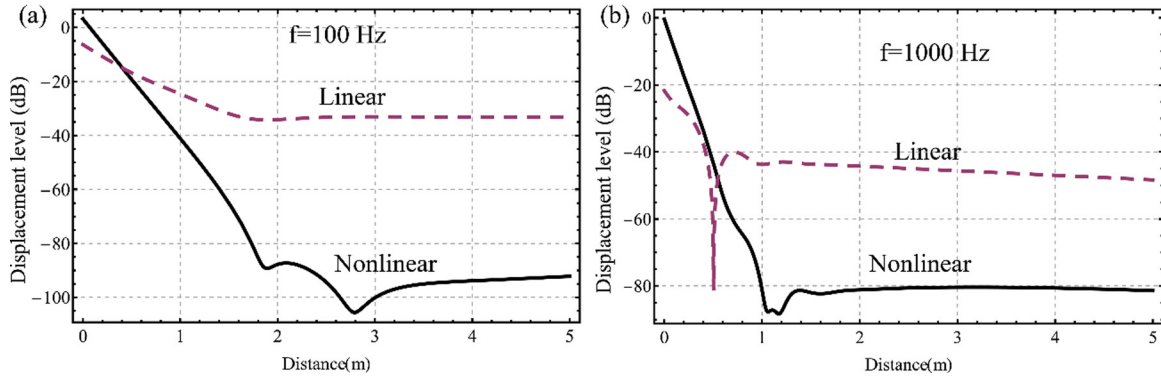
FIG. 4. (Color online) Variation of the nonlinear and linear displacement levels for different frequencies. The vertical axis is the ratio of the linear and nonlinear displacement amplitudes to the total displacement amplitude at $a = 0$.

is mainly contributed by $u_{NL}^{(1)}$ and $u_{NM}^{(1)}$ below the distance $a < 1.9$ m, and is then dominated by $u_{NF}^{(1)}$ when the distance exceeds 3.2 m because of the high attenuation of $u_{NL}^{(1)}$ and $u_{NM}^{(1)}$. For the 1000 Hz frequency response, the corresponding demarcation distances become $a = 1.1$ m and $a = 1.5$ m due to the greater attenuation of $u_{NL}^{(1)}$ and $u_{NM}^{(1)}$. At moderate distances, the amplitudes of these three waves are approximately equivalent. This again gives rise to obvious interference within this distance range. In addition, it is clear that the nonlinear displacement $u_{NF}^{(1)}$ exhibits a cumulative effect with increasing distance. This is a corollary of the quasi-non-dissipative system discussed in Sec. III. Here, it should be mentioned that the nonlinear displacement shown in Fig. 4 is contrary to the theoretical prediction of Donskoy and Khashanah (1997) at short distances. Their results showed a quasilinear growth of the nonlinear displacement with distance, which resulted from the assumption of a fully non-dissipative system. If a fully non-dissipative assumption is also applied to solve Eq. (28), it is predictable that a similar conclusion will be reached. However, extensive experimentation has shown that slow waves in a water-saturated sandy sediment are highly attenuated (Lee *et al.*, 2007; Kim and Yoon, 2009). Therefore, the non-dissipative assumption for the slow waves may lead to a significant error. The observed cumulative effect of nonlinear displacement amplitudes with distance in sandstone (Meegan *et al.*, 1993) is the result of the quasi-non-dissipative nature of that material. It is also found that the nonlinear displacement is greater than

the linear displacement at short distances, indicating considerable nonlinearity at such distances.

The relationship between the linear and nonlinear displacements for various distances is presented in Fig. 6. Strong nonlinearity is observed at short distances [a = 0.5 m, Fig. 6(a)], and the total displacement is dominated by $u_{NL}^{(1)}$ and $u_{NM}^{(1)}$. When the distance increases [a = 1 m, Fig. 6(b)], the amplitudes of $u_{NF}^{(1)}$, $u_{NL}^{(1)}$, and $u_{NM}^{(1)}$ become very similar. Hence, the interference of these waves results in fluctuation. When the distance continues to increase, the amplitudes of the nonlinear waves $u_{NL}^{(1)}$ and $u_{NM}^{(1)}$ are attenuated to negligible values, as indicated in Fig. 5, and the total nonlinear displacement becomes dominated by $u_{NF}^{(1)}$. For a longer distance (a = 50 m), both the linear and nonlinear displacements become negligible. In general, we conclude that the nonlinear displacement is dominated by $u_{NL}^{(1)}$ and $u_{NM}^{(1)}$ at short distances and in the low-frequency range, while it is dominated by $u_{NF}^{(1)}$ at long distances and the high-frequency range.

B. Nonlinear displacements generated by one-dimensional shear wave

The same material is used herein to investigate the nonlinear displacement generated by a shear wave. The displacement amplitude at the source point is again chosen as $A_s = 10^{-6}$m. From Fig. 7, a shear displacement wave with a frequency of 1000 Hz generates a strong nonlinear longitudinal wave for
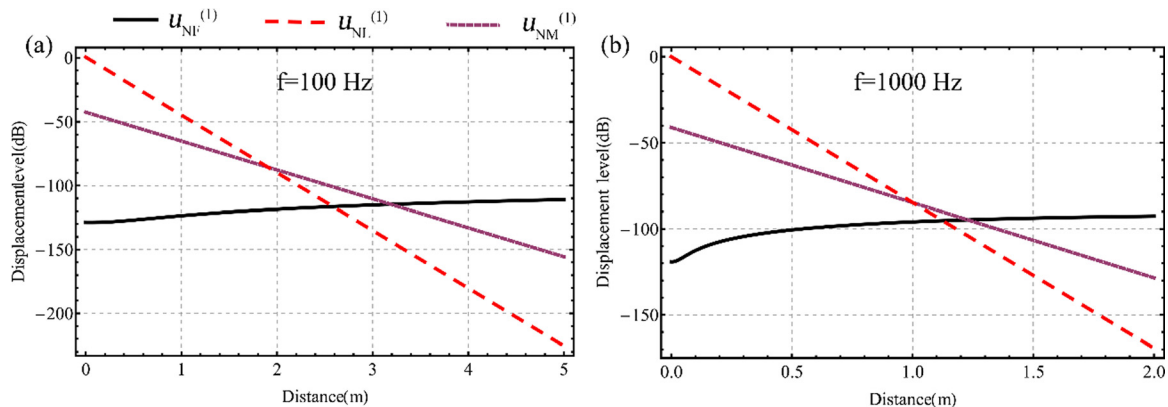
FIG. 5. (Color online) Variation of the nonlinear displacement levels of each nonlinear wave for different frequencies.
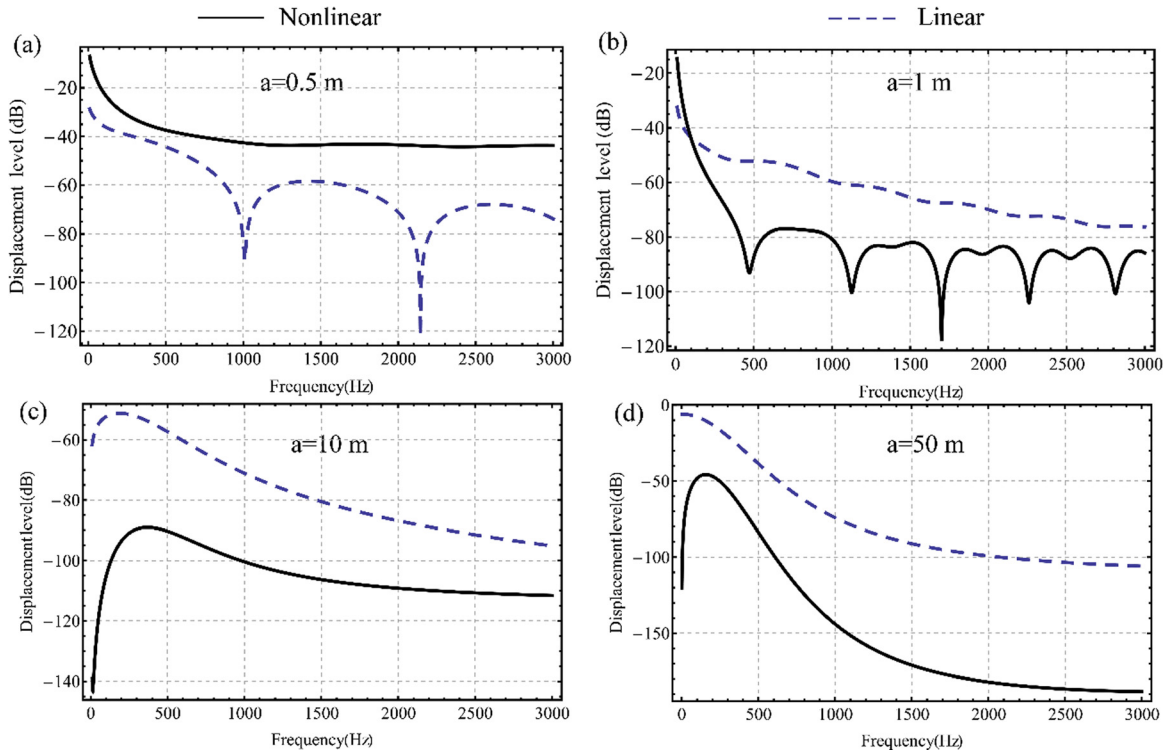
FIG. 6. (Color online) Variation of the nonlinear and linear displacement levels for various distance values. The vertical axis is the ratio of the linear and non-linear displacement amplitudes to the total displacement amplitude at $a = 0$.

the selected displacement amplitude. For a lower frequency shear wave ($f = 100$ Hz), the amplitude of the generated nonlinear longitudinal wave is significantly smaller. There is no major difference between the total nonlinear displacement and the fast nonlinear displacement u_{NF}, because the amplitudes of both the nonlinear displacements u_{NP} and u_{NL} are small. The nonlinear displacement contour levels for various distances and frequencies are also depicted in Fig. 8. It is clear that the nonlinear displacement gradually decreases with increasing distance. Nevertheless, strong interference is observed in the low-frequency region ($f < 100$ Hz). Considering the high attenuation of the slow nonlinear waves u_{NL}, the interference mainly occurs between the nonlinear waves u_{NF} and u_{NP}.

In general, the total nonlinear displacement field generated by a shear wave is mainly contributed by the fast nonlinear wave u_{NF} in the high-frequency range, while some interference occurs between u_{NF} and u_{NP} in the low-frequency range.

Equation (38) contains only one nonlinear elastic constant m. If the other linear elastic constants are known, it is easy to determine this nonlinear elastic constant by measuring the amplitude of the nonlinear waves experimentally. The remaining nonlinear elastic constants can then be determined by measuring the amplitude of the nonlinear waves generated by the linear fast and slow waves. However, the nonlinear elastic constant n disappears under the one-
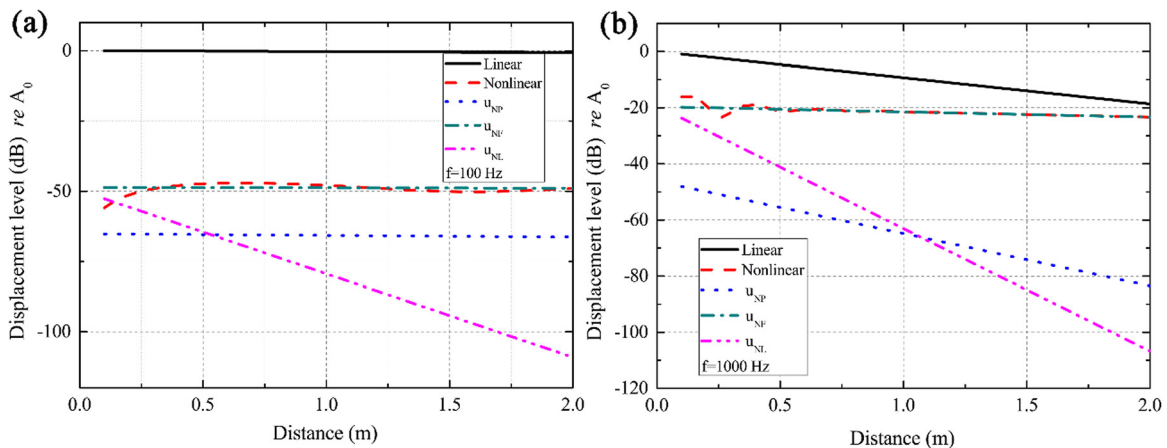
FIG. 7. (Color online) Nonlinear displacement levels generated by a shear wave for (a) the frequency at 100 Hz; and (b) the frequency at 1000 Hz. "Linear" means the linear displacement level of the linear shear wave. "Nonlinear" means the total nonlinear displacement level generated by the shear wave u_{NP}, u_{NF}, and u_{NL} in Eq. (39).

J. Acoust. Soc. Am. **142** (2), August 2017

Tong *et al.* 767
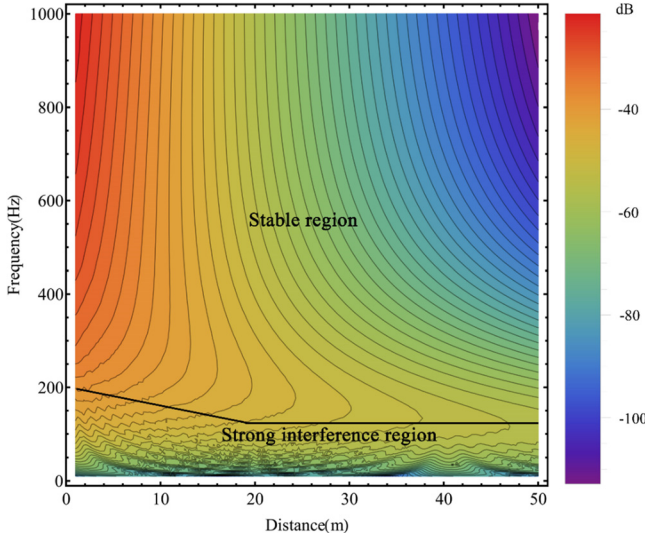
FIG. 8. (Color online) Nonlinear displacement levels (referred to A_s) generated by a shear wave. The difference of two neighboring lines is 2 dB.

dimensional assumption. Hence, the three-dimensional problem is needed, which may be studied in future works.

V. CONCLUSIONS

The nonlinear governing equations for saturated porous materials were established based on the Biot theory by introducing a set of nonlinear elastic constants into the Lagrangian formulation. In view of the complexity of the nonlinear governing equations in three dimensions, simple one-dimensional problems were put forward both for the case of a single one-dimensional longitudinal wave source and a single one-dimensional shear wave source. It was concluded that only double-frequency nonlinear longitudinal waves can be excited under the discussed cases. However, if the longitudinal and shear wave sources are coherently applied, both double-frequency nonlinear longitudinal and shear waves can be generated. To investigate a practical porous material, the nonlinear response of the displacement field was studied. It was found that the nonlinear displacement is dominated by the nonlinear slow wave in the near distance field while it gradually becomes dominated by the nonlinear fast wave in the far field. The nonlinear slow wave exhibits sharp attenuation with both increasing frequency and distance, while the nonlinear fast wave can propagate to long distances with only slight attenuation. For the nonlinear longitudinal wave generated by a shear wave, the attenuation performance differs depending on the frequencies and distances. The total nonlinear displacement field generated by a shear wave is mainly contributed by the fast nonlinear wave u_{NF} in the high-frequency range, while some interference occurs between the fast nonlinear wave u_{NF} and the nonlinear shear wave u_{NP} in the low-frequency range.

ACKNOWLEDGMENTS

APPENDIX

We assume that the time-dependent term for a linear wave is $e^{-j\omega t}$, then Eq. (21) can be rewritten as

$$\rho\omega^2 \bar{u}_1^{(0)} + \rho_f \omega^2 \bar{w}_1^{(0)} + (\lambda_c + 2\mu)\frac{\partial^2 \bar{u}_1^{(0)}}{\partial a^2}$$
$$+ \alpha M \frac{\partial^2 \bar{w}_1^{(0)}}{\partial a^2} = 0,$$
$$\rho_f \omega^2 \bar{u}_1^{(0)} + m'\omega^2 \bar{w}_1^{(0)} + j\omega\frac{\eta}{\kappa}\bar{w}_1^{(0)}$$
$$+ \alpha M \frac{\partial^2 \bar{u}_1^{(0)}}{\partial a^2} + M\frac{\partial^2 \bar{w}_1^{(0)}}{\partial a^2} = 0, \tag{A1}$$

where $u_1^{(0)} = \bar{u}_1^{(0)} e^{-j\omega t}$ and $w_1^{(0)} = \bar{w}_1^{(0)} e^{-j\omega t}$. Define two other notations

$$\beta_4 = -\frac{\alpha^2 M - (\lambda_c + 2\mu)}{\alpha m'\omega^2 + j\omega\dfrac{\alpha\eta}{\kappa} - \rho_f\omega^2},$$
$$\beta_5 = -\frac{\alpha\rho_f\omega^2 - \rho\omega^2}{\alpha m'\omega^2 + j\omega\dfrac{\alpha\eta}{\kappa} - \rho_f\omega^2}. \tag{A2}$$

From Eq. (A1), we obtain

$$\bar{w}_1^{(0)} = \beta_4 \frac{\partial^2 \bar{u}_1^{(0)}}{\partial a^2} + \beta_5 \bar{u}_1^{(0)}. \tag{A3}$$

Eliminating $\bar{w}_1^{(0)}$ from Eq. (A1), we derive the following fourth-order differential equation in terms of $\bar{u}_1^{(0)}$,

$$a_b \frac{\partial^4 \bar{u}_1^{(0)}}{\partial a^4} + b_b \frac{\partial^2 \bar{u}_1^{(0)}}{\partial a^2} + c_b \bar{u}_1^{(0)} = 0, \tag{A4}$$

where

$$a_b = \alpha M \beta_4,$$
$$b_b = (\lambda_c + 2\mu) + \alpha M \beta_5 + \rho_f \omega^2 \beta_4,$$
$$c_b = \rho_f \omega^2 \beta_5 + \rho\omega^2.$$

Equation (A4) is rewritten in another form as follows:

$$\left(\frac{\partial^2}{\partial a^2} + k_F^2\right)\left(\frac{\partial^2}{\partial a^2} + k_L^2\right)\bar{u}_1^{(0)} = 0, \tag{A5}$$

where k_F and k_L satisfy

$$k_F^2 + k_L^2 = \frac{b_b}{a_b},$$
$$k_F^2 \cdot k_L^2 = \frac{c_b}{a_b}. \tag{A6}$$

Solving Eq. (A5) and considering only waves propagating in the positive direction give

$$\bar{u}_1^{(0)} = A_0 e^{jk_F a} + B_0 e^{jk_L a}, \tag{A7}$$

where A_0 and B_0 are the amplitudes corresponding to the fast wave and the slow wave, respectively, which can be determined by the boundary conditions. Define the amplitude ratio of the fast wave to the slow wave as $R_{BA} = B_0/A_0$, then Eq. (A7) can be re-written as

$$\bar{u}_1^{(0)} = A_0 e^{jk_F a} + R_{BA} A_0 e^{jk_L a}. \tag{A8}$$

Substituting Eq. (A8) into Eq. (A3) gives

$$\bar{w}_1^{(0)} = \lambda_F A_0 e^{jk_F a} + R_{BA} \lambda_L A_0 e^{jk_L a}, \tag{A9}$$

where $\lambda_i = (\beta_5 - \beta_4 k_i^2)\ (i = F, L)$.

As an illustrative example is given below, the value of R_{BA} can be estimated. As shown in Fig. 9, a wave is excited on the left boundary of a plate. Assume that the wave is a one-dimensional plane wave, then the wave field in the body of the plate can be expressed as

$$u_p(a, t) = A_p e^{j(k_p a - \omega t)} + B_p e^{j(-k_p a - \omega t)}, \tag{A10}$$

where k_p is the wave number. Consider the saturated soil that is a semi-infinite medium, the wave field can be expressed by Eq. (A7). The displacement and stress on the interface of the soil and plate should satisfy the continuity condition, i.e., $u_p(0, t) = u_1(0, t)$ and $\sigma_p(0, t) = \sigma_1(0, t)$, where σ_p and σ_1 are the stress fields of the plate and porous soil, respectively. According to the work of Biot (1962), the stress of the porous soil is

$$\sigma_1 = (\lambda_c + 2\mu)u_{1,a} + \alpha M w_{1,a}, \tag{A11}$$

under the one-dimensional assumption. The stress of the plate can be expressed as

$$\sigma_p = E_p u_{p,a}, \tag{A12}$$
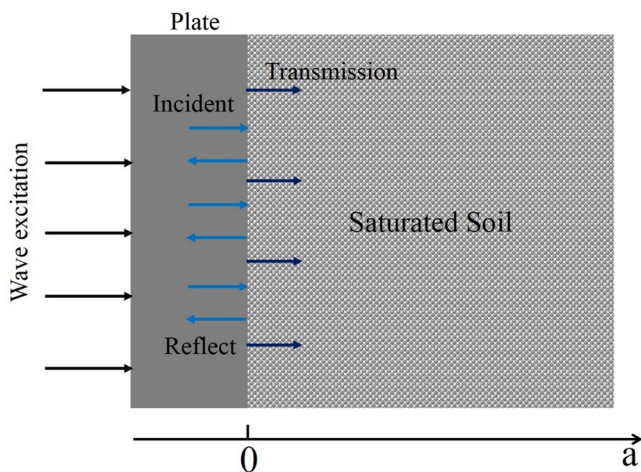
FIG. 9. (Color online) Schematic of a wave transmission from a plate to a medium of saturated soil.

where E_p is the modulus of the plate. Substituting Eqs. (A7), (A10), (A11), and (A12) into the boundary conditions at the interface of the plate and the soil, the coefficients A_0 and B_0 can be solved as

$$A_0 = \frac{E_L k_L (A_p + B_p) + E_p k_p (B_p - A_p)}{E_L k_L - E_F k_F},$$
$$B_0 = \frac{-E_F k_F (A_p + B_p) - E_p k_p (B_p - A_p)}{E_L k_L - E_F k_F}, \tag{A13}$$

where $E_i = \lambda_c + 2\mu + \lambda_i \alpha M\ (i = F, L)$. From a practical engineering point of view, the modulus of the plate (e.g., reinforced concrete walls) is greatly larger than that of soil. It corresponds to that wave transmission from a stiff material into a soft material. It is well known that the values of A_p and B_p are approximately equal to each other. As a result,

$$B_0/A_0 \approx -\frac{E_F k_F}{E_L k_L} \tag{A14}$$

can be estimated.

Ashby, M. F. (**2006**). "The properties of foams and lattices," Philos. Trans. A. Math. Phys. Eng. Sci. **364**, 15–30.

Berryman, J. G., and Thigpen, L. (**1985**). "Nonlinear and semilinear dynamic poroelasticity with microstructure," J. Mech. Phys. Solids **33**, 97–116.

Biot, M. A. (**1941**). "General theory of three-dimensional consolidation," J. Appl. Phys. **12**, 155–164.

Biot, M. A. (**1956a**). "Theory of propagation of elastic waves in a fluid-saturated porous solid. 1. Low-frequency range," J. Acoust. Soc. Am. **28**, 168–178.

Biot, M. A. (**1956b**). "Theory of propagation of elastic waves in a fluid-saturated porous solid. 2. Higher frequency range," J. Acoust. Soc. Am. **28**, 179–191.

Biot, M. A. (**1962**). "Mechanics of deformation and acoustic propagation in porous media," J. Appl. Phys. **33**, 1482–1498.

Biot, M. A. (**1973**). "Nonlinear and semilinear rheology of porous solids," J. Geophys. Res. **78**, 4924–4937, doi:10.1029/JB078i023p04924.

Borja, R. I., and Alarcón, E. (**1995**). "A mathematical framework for finite strain elastoplastic consolidation Part 1: Balance laws, variational formulation, and linearization," Comput. Meth. Appl. Mech. Eng. **122**, 145–171.

Bouzidi, Y., and Schmitt, D. R. (**2009**). "Measurement of the speed and attenuation of the Biot slow wave using a large ultrasonic transmitter," J. Geophys. Res. **114**, B08201, doi:10.1029/2008JB006018.

Cui, Z. W., Liu, J. X., Wang, C. X., and Wang, K. X. (**2010**). "Elastic waves in Maxwell fluid-saturated porous media with the squirt flow mechanism," Acta Phys. Sin. **59**, 8655–8661.

Cui, Z. W., Liu, J. X., and Wang, K. X. (**2003**). "Elastic waves in non-Newtonian (Maxwell) fluid-saturated porous media," Wave Random Media **13**, 191–203.

Dazel, O., and Tournat, V. (**2010**). "Nonlinear Biot waves in porous media with application to unconsolidated granular media," J. Acoust. Soc. Am. **127**, 692–702.

Donskoy, D. M., Khashanah, K., and McKee, T. G. (**1997**). "Nonlinear acoustic waves in porous media in the context of Biot's theory," J. Acoust. Soc. Am. **102**, 2521–2528.

Johnson, P. A., and Jia, X. (**2005**). "Nonlinear dynamics, granular media and dynamic earthquake triggering," Nature **437**, 871–874.

Johnson, P. A., Savage, H., Knuth, M., Gomberg, J., and Marone, C. (**2008**). "Effects of acoustic waves on stick-slip in granular media and implications for earthquakes," Nature **451**, 57–60.

Kempa, M. (**1997**). "On the description of the consolidation phenomenon by means of a two-component continuum," Arch. Mech. **49**, 893–917.

Kim, B.-N., and Yoon, S. W. (**2009**). "Nonlinear parameter estimation in water-saturated sandy sediment with difference frequency acoustic wave," Ultrasonics **49**, 438–445.

Larsson, J., and Larsson, R. (**2002**). "Non-linear analysis of nearly saturated porous media: Theoretical and numerical formulation," Comput. Meth. Appl. Mech. Eng. **191**, 3885–3907.

Lee, K. I., Humphrey, V. F., Kim, B. N., and Yoon, S. W. (**2007**). "Frequency dependencies of phase velocity and attenuation coefficient in a water-saturated sandy sediment from 0.3 to 1.0 MHz," J. Acoust. Soc. Am. **121**, 2553–2558.

Legland, J.-B., Tournat, V., Dazel, O., Novak, A., and Gusev, V. (**2012**). "Linear and nonlinear Biot waves in a noncohesive granular medium slab: Transfer function, self-action, second harmonic generation," J. Acoust. Soc. Am. **131**, 4292–4303.

Liu, Y., Liu, K., Gao, L. T., and Yu, T. X. (**2005**). "Characteristic analysis of wave propagation in anisotropic fluid-saturated porous media," J. Sound. Vib. **282**, 863–880.

Lopatnikov, S. L., and Cheng, A. H. D. (**2004**). "Macroscopic Lagrangian formulation of poroelasticity with porosity dynamics," J. Mech. Phys. Solids **52**, 2801–2839.

Meegan, G. D., Johnson, P. A., Guyer, R. A., and McCall, K. R. (**1993**). "Observations of nonlinear elastic wave behavior in sandstone," J. Acoust. Soc. Am. **94**, 3387–3391.

Moussatov, A., Castagnède, B., and Gusev, V. (**2001**). "Observation of non-linear interaction of acoustic waves in granular materials: Demodulation process," Phys. Lett. A **283**, 216–223.

Papargyri-Beskou, S., Polyzos, D., and Beskos, D. E. (**2012**). "Wave propagation in 3-D poroelastic media including gradient effects," Arch. Appl. Mech. **82**, 1569–1584.

Plona, T. J. (**1980**). "Observation of a second bulk compressional wave in a porous-medium at ultrasonic frequencies," Appl. Phys. Lett. **36**, 259–261.

Porubov, A. V., and Maugin, G. A. (**2009**). "Cubic non-linearity and longitudinal surface solitary waves," Int. J. Nonlin. Mech. **44**, 552–559.

Pushkina, N. I. (**2012**). "Nonlinear three-wave interaction in marine sediments," Phys. Wave Phenomena **20**, 204–207.

Rice, J. R. (**1975**). "On the stability of dilatant hardening for saturated rock masses," J. Geophys. Res. **80**, 1531–1536, doi:10.1029/JB080i011p01531.

Sharma, M. D. (**2007**). "Wave propagation in a general anisotropic poroelastic medium: Biot's theories and homogenisation theory," J. Earth. Syst. Sci. **116**, 357–367.

Solovev, V. (**1990**). "Experimental investigation of non-linear seismic effects," Phys. Earth Planet. Inter. **62**, 271–276.

Tao, H. B., Liu, G. B., Xie, K. H., Zheng, R. Y., and Deng, Y. B. (**2014**). "Characteristics of wave propagation in the saturated thermoelastic porous medium," Transport Porous Med. **103**, 47–68.

Tong, L., Yu, Y., Hu, W., Shi, Y., and Xu, C. (**2016**). "On wave propagation characteristics in fluid saturated porous materials by a nonlocal Biot theory," J. Sound. Vib. **379**, 106–118.

Wang, X., Peng, F., and Chang, B. (**2009**). "Sound absorption of porous metals at high sound pressure levels," J. Acoust. Soc. Am. **126**, EL55–EL61.

Wilmanski, K. (**1996**). "Porous media at finite strains-The new model with the balance equation for porosity," Arch. Mech. **48**, 591–628.

Yang, D. X., Li, Q., and Zhang, L. Z. (**2015**). "Propagation of pore pressure diffusion waves in saturated porous media," J. Appl. Phys. **117**, 134902.

Zhang, B., Chen, T., Zhao, Y., Zhang, W., and Zhu, J. (**2012**). "Numerical and analytical solutions for sound propagation and absorption in porous media at high sound pressure levels," J. Acoust. Soc. Am. **132**, 1436–1449.

Zhu, Z., Roos, M. S., Cobb, W. N., and Jensen, K. (**1983**). "Determination of the acoustic nonlinearity parameter B/A from phase measurements," J. Acoust. Soc. Am. **74**, 1518–1521.